Power management strategy derived from optimal control: Application to Fuel Cell Hybrid powertrains

ARTICLE *in* CONTROL ENGINEERING PRACTICE · APRIL 2010

Impact Factor: 1.81

4 AUTHORS, INCLUDING:

Sebastien Delprat

University of Valenciennes and Hainaut-Ca…

57 PUBLICATIONS **909** CITATIONS

SEE PROFILE

Thierry-Marie Guerra

University of Valenciennes and Hainaut-Ca…

215 PUBLICATIONS **3,739** CITATIONS

SEE PROFILE

Felix N. Büchi

Paul Scherrer Institut

110 PUBLICATIONS **2,368** CITATIONS

SEE PROFILE

Fuel Efficient Power Management strategy for Fuel Cell Hybrid powertrains.

J. Bernard[1], S. Delprat[2, 3,4], T.M. Guerra[2, 3,4], F.N. Büchi[1]

[1] Electrochemistry Laboratory, Paul Scherrer Institut, 5232 Villigen-PSI, Switzerland,

{jerome.bernard; felix.buechi}@psi.ch

[2] Univ Lille Nord de France, F-59000 Lille, France
[3] UVHC, LAMIH, F-59313 Valenciennes, France
[4] CNRS, UMR 8530, F-59313 Valenciennes, France
{delprat,guerra}@univ-valenciennes.fr

Abstract

A real time control strategy for Fuel Cell Hybrid Vehicles is proposed. The objective is to reduce the hydrogen consumption by using an efficient power sharing strategy between the fuel cell system (FCS) and the energy buffer (EB). The energy buffer (battery or supercapacitor) is charge-sustained (no plug-in capabilities). The real time control strategy is derived from a non-causal optimization algorithm based on optimal control theory. The strategy is validated experimentally with a Hardware-in-the-Loop (HiL) test bench based on a 600W fuel cell system.

Keyword: Hybrid vehicle; Fuel Cell System; Optimal Control; Real Time Control; Experimental Results; Test Bench

1. Introduction

Fuel cell hybrid vehicles are using two energy sources to supply their electric powertrain /Dietrich et al. 2003/ /Yamaguchi 2003/. The primary power source is a polymer electrolyte fuel cell (PEFC) system where the fuel cell stack converts hydrogen and oxygen into electric energy with water and heat as the by-products /Gruber & al. 2009/ /Wee 2007/. The second

energy source is the energy buffer which is power reversible. Usually, batteries (lead-acid, Ni-MH, Li-ion) /Spotnitz 2005/ or supercapacitors /Barrade et Rufer 2004/ are under interest to hybridize the fuel cell system /Bauman et Mehrdad 2008/. The two fundamental roles of the energy buffer are /Jeong et Oh 2002/ /Markel et al. 2003/:

- to recover the braking energy;
- to power-assist the fuel cell system when its rated power is insufficient or its power rate capability doesn't match the transient power demand.

Since the power source is hybrid, a power management strategy is needed to define the power sharing between the fuel cell system and the energy buffer. Usually, for hybrid vehicles without plug-in capabilities, the power management strategy should reduce the fuel consumption while keeping the state of charge (SOC) of the energy buffer within reasonable bounds. This paper focuses on the control strategy problem.

For hybrid vehicles, the control strategies are classified into 2 categories /Guezennec et al. 2003/ /Rodatz et al. 2005/: **case 1)** non-causal when the future driving cycle is completely known and **case 2)** causal when the future is unknown. In the first case, the strategies may provide an optimal solution leading to the lowest fuel consumption, but they are unusable for real time applications. Such strategies may be obtained using the minimum principle /Serrao et al. 2009/ or dynamic programming approaches /Scordia 2004/. In the latter case, the strategies can be used online for vehicle real time control but are necessarily sub-optimal. Several approaches have been considered. Let us quote the Losses Minimization Strategy /Seiler et Schröder 1998/ minimizes the powertrain losses at each sampling time and an adaptive control law /Dalvi & al. 2009/. The family of Equivalent Consumption Minimization Strategies (ECMS) consider a criterion composed of the hydrogen consumption and the

weighted electric power consumption /Sciarretta et al. 2004/ /Musardo et al. 2005/; the key point being the choice of the weighting factor. This paper investigates an approach somehow similar to ECMS to derive an efficient real time control strategy (case 2) from the optimal solution (case 1). The main point is that weighting factor adaptation is not dependent on the *time ordered* prediction of the future power demand but only on its *distribution*. This important aspect allows adapting this parameter without requiring a complex prediction algorithm.

In the first part of the paper, the optimization problem is formulated. It consists in minimizing the hydrogen consumption of the fuel cell system under several constraints (power limits, system dynamics, etc.). Based on this problem formulation, control strategies are investigated in the second part. Especially, a real time control strategy is derived from an optimal control algorithm. Finally in the third part, the real time control strategy proposed is validated experimentally on a HiL (Hardware in the Loop) test bench emulating a fuel cell hybrid vehicle on a reduced scale. A 600W PEM fuel cell system and a 12V/18Ah lead acid battery are used. The conclusions highlight the perspectives launched in the present paper.

2. Problem formulation

In the following, the equations are expressed in discrete time. The sampling time is T_s and k the sample number. For simulation purposes, a 1500 kg duty vehicle propelled by a 75 kW electric machine is considered. Its hybrid energy source is composed by a 40 kW fuel cell system coupled with a 120V-28Ah Ni-MH battery. This vehicle is referred to as *Vehicle1*. Two models are used thereinafter. The first one, *Model1*, is an energetic model used only for simulations purposes; it is an "Advisor-like" detailed model /Haraldsson et Wipke 2004/ /Boettner et al. 2002/. The second one, *Model2*, is a simplified model only used to derive the control laws. Differences between the models concern mainly the battery modeling. For the simulation model *Model1*, the battery is modeled as a non linear current integrator. For

Model2, considering the electric bus topology and the power converters, the battery is modeled as a power integrator. Therefore the derivation of the control laws is easier.

Only *Model2* is presented here. For more details concerning the models and their validity, the reader may refer to /Bernard 2007/. The upper part of fig. 6 provides a comparison between *Model1* and *Model2*.

- **Power flows**

Considering the powertrain arrangement of a hybrid fuel cell vehicle, fig. 1, the electric bus receives the positive power P_{FCS} from the fuel cell system and the power P_{EB} from the energy buffer ($P_{EB} > 0$ in discharge, and $P_{EB} < 0$ in charge). The power demand P_{DEM} corresponds to the power requested by the electric motor to propel the vehicle ($P_{DEM} > 0$ during traction phases and $P_{DEM} < 0$ during kinetic energy recovering). For convenience, the power converters are implicitly taken into account in the efficiencies of the fuel cell system, energy buffer and electric motor(s). The electric node (Fig. 1) imposes the following equation:

$$P_{FCS}(k) + P_{EB}(k) = P_{DEM}(k) \tag{1}$$

Since the power demand $P_{DEM}(k)$ in eq. (1) is known for each sample k, it is obvious that it is enough to define one power (P_{FCS} or P_{EB}). The fuel cell system power P_{FCS} is set as the decision variable.

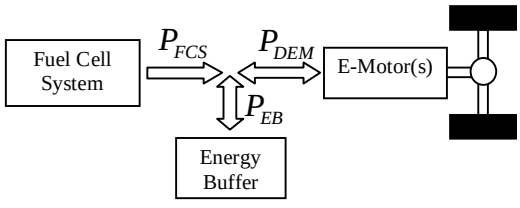

Fig. 1. Energy flows in the powertrain.

- **Energy buffer (battery or supercapacitor)**

The energy buffer is considered as a power integrator:

$$X(k+1) = X(k) - Q\left(P_{EB}(k)\right) \cdot T_s \tag{2}$$

with T_s the sampling period and X the energy stored. The power P_{EB} is bounded as:

$$\underline{P_{EB}}\left(X(k)\right) \le P_{EB}(k) \le \overline{P_{EB}}\left(X(k)\right) \tag{3}$$

In eq. (2), Q expresses the gross (respectively net) power drained from (respectively supplied to) the energy buffer. This map may be either measured on a test bench or computed using battery and power converter models. It integrates the power losses induced by the internal resistance, the faradic efficiency, and eventually the power converter. Some approximations may be required to compute the map Q, for example for a battery, an average faradic efficiency may be considered. An example of Q is given fig. 2.

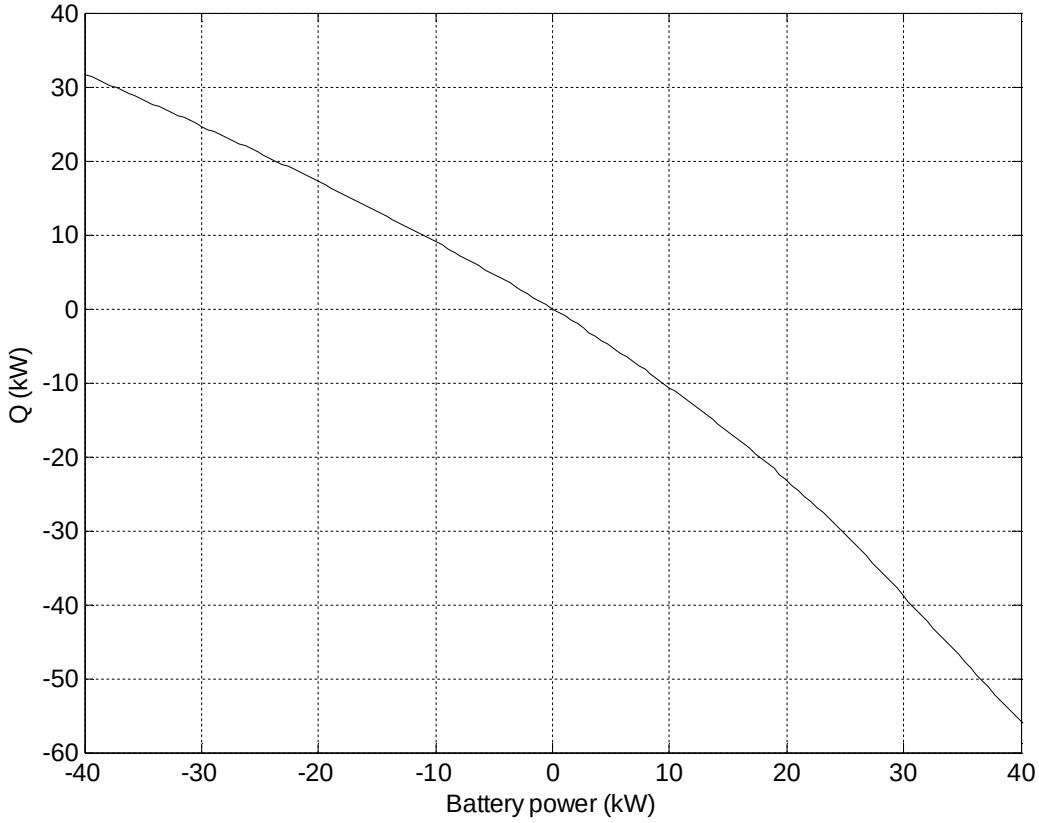

Fig. 2. Example of Q map for a 40kW Ni-MH battery.

When substituting eq. (1) into eq. (2), X is expressed as a function of the fuel cell system power P_{FCS}:

$$X(k+1) = X(k) - Q\left(P_{DEM}(k) - P_{FCS}(k)\right)\cdot T_s \tag{4}$$

- **Fuel cell system**

The objective is to obtain an efficient power split which minimizes the hydrogen consumption. Thus, the quantity to minimize is:

$$J = \sum_{k=0}^{N} \dot{m}_{H_2}\left(P_{FCS}(k)\right)\cdot T_s \ , \tag{5}$$

with $N\cdot T_s$ the driving cycle duration. In eq. (5), $\dot{m}_{H_2}$ is the instantaneous hydrogen consumption (g/s) which is related to the operating conditions, i.e. pressure, stoichiometry, membranes humidity, stack temperature, and the consumption of the auxiliary components. An example of $\dot{m}_{H_2}$ is illustrated in fig. 3 for a 40kW fuel cell system under nominal operating conditions; $\dot{m}_{H_2}$ is a function of the fuel cell system power P_{FCS}, which is bounded:

$$\underline{P_{FCS}} \le P_{FCS}(k) \le \overline{P_{FCS}} \tag{6}$$

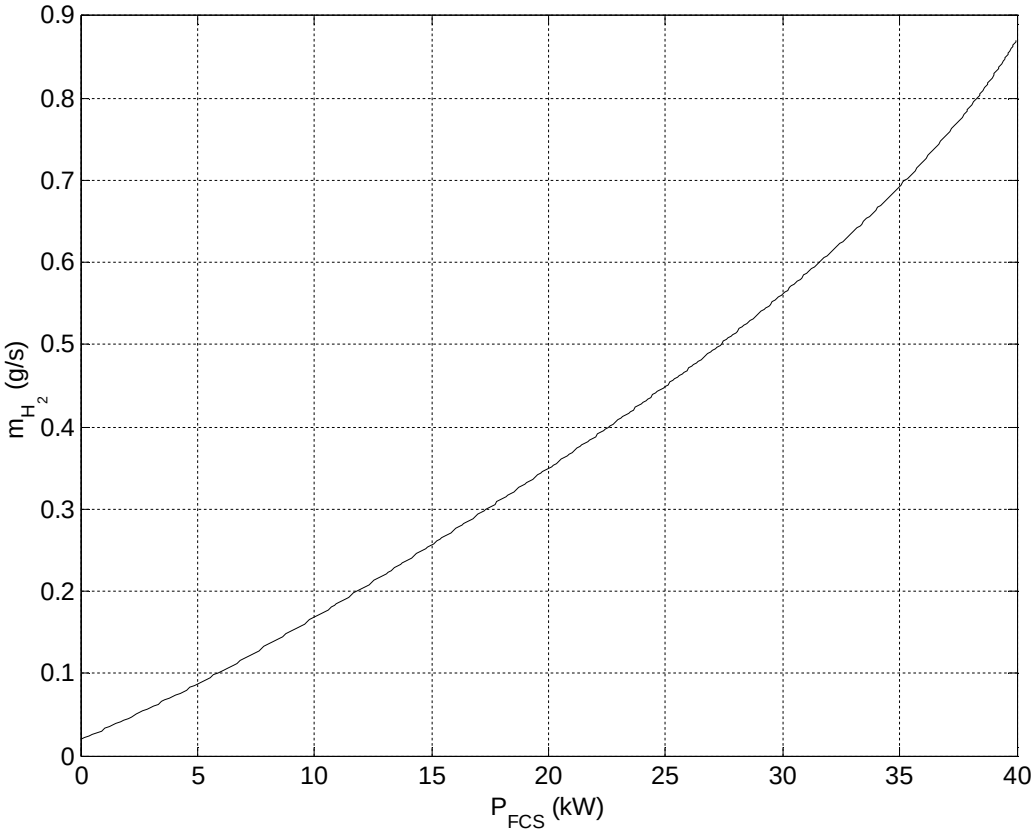

Fig. 3. Example of instantaneous hydrogen consumption as function of the fuel cell system power.

Considering the power limitation of the energy buffer eq. (3) and the equality constraint eq. (1), the set of admissible values for the fuel cell system power P_{FCS} is defined as:

$$A(k) \le P_{FCS}(k) \le B(k) \tag{7}$$

with

$$A(k) = \max\left\{\underline{P_{FCS}}, P_{DEM}(k) - \overline{P_{EB}}\left(X(k)\right)\right\} \tag{8}$$

$$B(k) = \min\left\{\overline{P_{FCS}}, P_{DEM}(k) - \underline{P_{EB}}\left(X(k)\right)\right\} \tag{9}$$

At last a constraint on the final state of charge is added:

$$X(N) = X(0) + \Delta X_{sp} \tag{10}$$

According to (10), the system state should reach a prescribed value $X(0) + \Delta X_{sp}$ at the end of the driving cycle, with ΔX_{sp} being a chosen global state variation.

- **Problem formulation**

According to the equations describing the fuel cell system and the energy buffer, the problem to solve is:

- ***Criterion:***

$$J = \sum_{k=0}^{N} \dot{m}_{H_2}\left(P_{FCS}\left(k\right)\right) \cdot T_s \tag{5}$$

- ***System:***

$$X\left(k+1\right) = X\left(k\right) - Q\left(P_{DEM}\left(k\right) - P_{FCS}\left(k\right)\right) \cdot T_s \tag{4}$$

- ***Constraints:***

$$A\left(k\right) \le P_{FCS}\left(k\right) \le B\left(k\right) \tag{11}$$

$$X\left(N\right) = X\left(0\right) + \Delta X_{sp} \tag{12}$$

3. Control strategies

3.1. Off-line optimal solution

Off-line optimal solutions are obtained with optimal control algorithms. These algorithms use an a priori known driving cycle, so they are referred to as non-causal approaches. However, the results obtained should be considered as useful benchmarks for analyzing, evaluating and deriving real-time control strategies. For the considered problem, two main optimal control approaches have been considered /Scordia 2004/ : 1) the ***discrete dynamic programming*** provides a numerical solution by considering the Hamilton-Bellman-Jacobi (HBJ) equation and a quantified state variable, and 2) the ***minimum principle*** provides a formal expression of the necessary optimality conditions /Pontryagin et al. 1962/. The second method is considered in this paper.

- **Minimum principle**

With the classical minimum principle, necessary optimality conditions may be found /Delprat et al. 2004/ /Bernard et al. 2006/ /Sciaretta et Guzzella 2007/. The system dynamics equality constraint (4) is introduced into criterion (5) using Lagrange parameters $\lambda(k)$ to form the Hamiltonian H:

$$H(k) = \dot{m}_{H_2}\left(P_{FCS}(k)\right)\cdot T_s - \lambda(k+1)\cdot\left[X(k) - Q\left(P_{DEM}(k) - P_{FCS}(k)\right)\cdot T_s\right] \quad (13)$$

Along the optimal trajectory, the Lagrange parameters $\lambda(k)$ verify the following condition:

$$\frac{\partial H(k)}{\partial X(k)} = -\lambda(k),\ k \in \{0...N\} \quad (14)$$

Equation (14) directly leads to $\lambda(k+1) = \lambda(k)$, which means that the optimal solution is achieved for a constant value $\lambda(k) = \lambda_0$. Thus considering $\lambda(k) = \lambda_0$ and eq. (13), the decision variable P_{FCS} is obtained by minimizing the Hamiltonian for $k \in \{0...N\}$:

$$P_{FCS}(k) = \underset{A(k)\le P_{FCS}(k)\le B(k)}{\arg\min}\left(\dot{m}_{H_2}\left(P_{FCS}\right) - \lambda_0\cdot Q\left(P_{DEM}(k) - P_{FCS}\right)\right) = \Pi\left(P_{DEM}(k), \lambda_0\right) \quad (15)$$

Therefore, it appears in (15) that the only tuning parameter remaining is the initial value of the Lagrange parameter λ_0.

- **Influence of λ_0**

The power demand P_{DEM} depends on the vehicle/powertrain specifications and the driving cycle. For a given λ_0, to satisfy this power demand, the control decision P_{FCS} is calculated with eq. (15). Nevertheless, since $\lambda_0 \in \mathbb{R}$, it exists an infinite number of control trajectories derived from eq. (15) leading to infinite possible state evolutions. Let us define $\Delta X = X(N) - X(0)$ the overall state variation.

For instance, for vehicle *Vehicle1* driving the outer-urban cycle "R3" /André et al. 2006/, two different values of λ_0 have been considered, fig. 4. The lower value ($\lambda_0 = 1.6 \times 10^{-5}$) exploits few power from the fuel cell system which leads to a progressive discharge of the battery ($\Delta X = -29\%$), whereas the higher value ($\lambda_0 = 2.1 \times 10^{-5}$) makes the fuel cell system more active which leads to a gradual recharge of the battery ($\Delta X = +22\%$). The hydrogen consumption is also lower in the first case (0.97 kg/100km) than in the second case (1.83 kg/100km).

Thus λ_0 is the only parameter that may be exploited to reach the final state set point specified by (12).

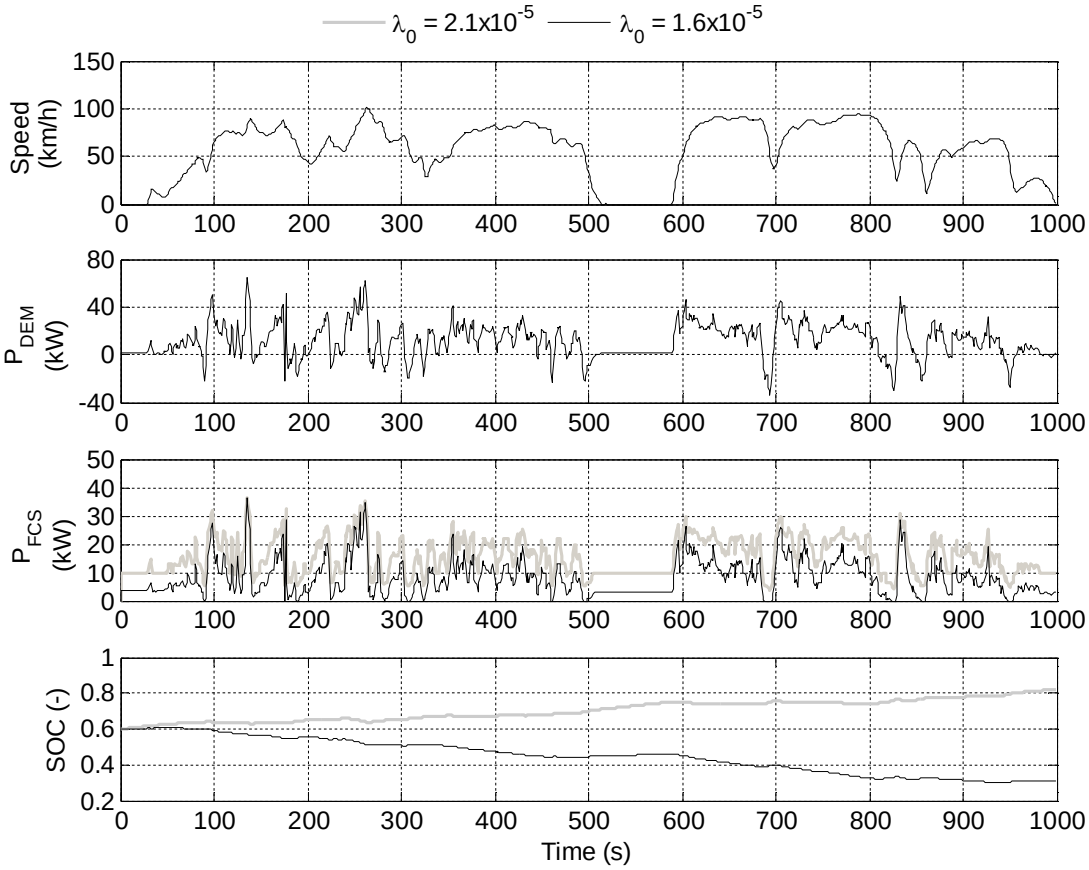

Fig. 4. Example of results on the R3 driving cycle for *Vehicle1*.

- **Global constraint ΔSOC to fix λ_0**

Equation (2) is a simplified battery model used to derive the optimal control law. In simulation, for a given λ_0, controls are obtained using (15) and applied to a more detailed model (namely *Model1)*. For example, upper part of fig. 6 illustrates the actual variation of the battery state of $SOC(N) - SOC(0)$ as a function of λ_0. Since *Model2*, and particularly equation (2) is a simplified version of *Model1*, the constraint should not be added on the variable $X(k)$ equation (2), but on the simulated battery state of charge $SOC(k)$ issued from *Model1*. Therefore, in practice constraint (12) is replaced with:

$$SOC(N) = SOC(0) + \Delta SOC_{sp} \tag{16}$$

with ΔSOC_{sp} a balance target of the state of charge.

Considering the upper part of fig. 6, the corresponding value of λ_0 satisfying (16) is easily obtained through successive simulations using a dichotic search /Delprat et al. 2004/ /Bernard et al. 2006/. In this case the power demand (or the driving cycle) is a priori known to perform successive iterations. Thus, by fixing the value of ΔSOC_{sp}, the approach is non-causal and can be only used off-line. For the sake of convenience, this algorithm will be referred to as *"offline optimization" algorithm.*

- **Estimation of $\widehat{\Delta SOC}$ and $\widehat{\lambda_0}$**

Finding the value of λ_0 leading to a prescribed ΔSOC_{sp} may require high computational efforts due to the necessity of several simulations. The present section explains how to reduce the computation time using an approximation $\widehat{\Delta SOC}$ of $SOC(N)-SOC(0)$. First, an approximation of the battery state of charge is considered:

$$\widehat{SOC} = \frac{X}{X_{\max}} \tag{17}$$

with X an energy and $X_{\max}$ the maximal energy level of the battery.

The energy balance ΔX can be calculated using (4) and (15):

$$\Delta X = T_s \cdot \sum_{k=0}^{N} Q\left(P_{DEM}(k) - \Pi\left(P_{DEM}(k), \lambda_0\right)\right) \tag{18}$$

Considering (17) and (18), an approximation of the variation of the state of charge $SOC(N)-SOC(0)$ is:

$$\widehat{\Delta SOC} = f(\lambda_0) \tag{19}$$

with $f(\lambda_0) = \frac{T_s}{X_{\max}} \cdot \sum_{k=0}^{N} Q\left(P_{DEM}(k) - \Pi\left(P_{DEM}(k), \lambda_0\right)\right)$

For large values of N, using (19) to find λ_0 satisfying (16) may still require a lot of computational efforts. A simpler but approximated expression of $f(\lambda_0)$ may be derived

considering the power demand histogram. Let n_i be the number of power demand values $P_{DEM}(k), k = 0..N$, that belongs to the i^{th} bin. Each bin is represented by its average value P_{DEM}^i.

Therefore the variation of the state of charge is approximated by:

$$\widehat{\Delta SOC}' = \hat{f}(\lambda_0) \tag{20}$$

with $\hat{f}(\lambda_0) = \frac{T_s}{X_{\max}} \cdot \sum_{i=1}^{C} n_i \cdot Q\left(P_{DEM}^i - \Pi\left(P_{DEM}^i, \lambda_0\right)\right)$ and C the number of bins.

Fig. 6 represents the actual value of $Q\left(P_{DEM}(k) - \Pi\left(P_{DEM}(k), \lambda_0\right)\right)$ and the approximation used $Q\left(P_{DEM}^i - \Pi\left(P_{DEM}^i, \lambda_0\right)\right)$ for the particular case $\lambda_0 = 3.7 \cdot 10^{-5}$ and $C = 33$.

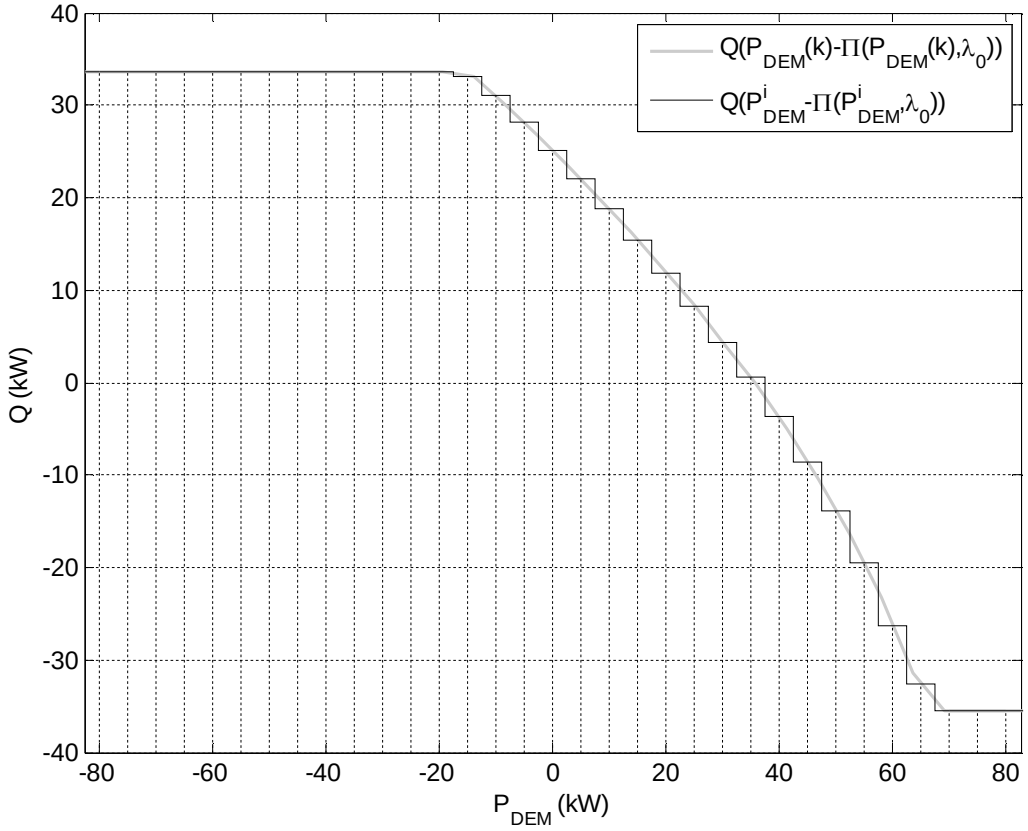

Fig. 5. Comparison of $Q\left(P_{DEM}(k) - \Pi\left(P_{DEM}(k), \lambda_0\right)\right)$ and its approximation $Q\left(P_{DEM}^i - \Pi\left(P_{DEM}^i, \lambda_0\right)\right)$ for the particular case $\lambda_0 = 3.7 \cdot 10^{-5}$

To validate the proposed approximation, $\widehat{\Delta SOC}'$ has been estimated according to eq. (20) with $C = 33$ and is compared to the actual value $\Delta SOC = SOC(N) - SOC(0)$ obtained by the simulation model *Model1* for several values of λ_0, fig. 6. Let us recall that for *Model1*,

ΔSOC is calculated by current integration in a more detailed model, whereas in *Model2* $\widehat{\Delta SOC}'$ is estimated using a rather simple model (20). The estimation error remains below 1 % for the R3 driving cycle. Therefore eq. (20) provides a sufficiently good and fast estimation of ΔSOC.

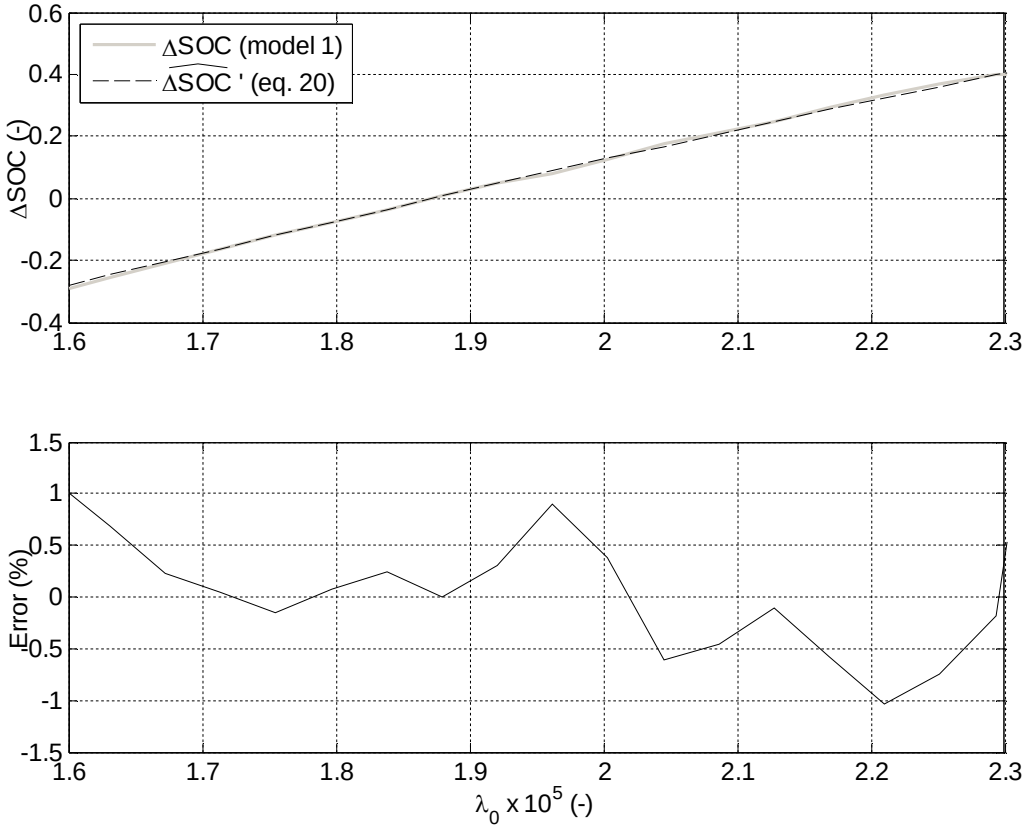

Fig. 6. Comparison of ΔSOC as a function of λ_0 using *Model1* and its approximation using eq. (20)

Table 1 shows the computation time of the dichotic search using the *Model1* and the simplified version using approximation (20) for different cycles provided by the Artemis study /André et al. 2006/. The computer used was a desktop PC with a core 2 duo 3Ghz processor and 2Go of RAM. In all cases, the same initial value of $\lambda_0 = 10^{-5}$ is used in the dichotic search. The algorithm is stopped as soon as the desired variation of the state of charge is achieved within a $\varepsilon_{soc} = 0.1\%$ tolerance.

The computation time for the estimation of λ_0 using the approximation is significantly reduced and remains around 0.4s. For cycles having similar length, the computation time for the dichotic search may vary slightly according to the number of iterations required to reach the desired state of charge balance with the desired accuracy. The computation time for the estimation of λ_0 using equation (20) depends mainly on the number of bins in the power distribution whereas the cycle length has a minor influence.

Cycle name	NEDC	UF3	R3	A1
Cycle time	1180s	1066s	1000s	733s
Computation time using *Model1*	11.3s	11.7s	14.6s	14.1s
Computation time using equation (20)	0.38s	0.39s	0.39s	0.43s

Table 1: Computation time for a dichotic search and an estimation of the parameter λ.

The real time strategy described in the next section is based on the estimation of $\widehat{\Delta SOC}'$ using equation (20).

3.2. On-line real time strategy

As previously discussed, keeping the Lagrange parameter constant $\lambda(k) = \lambda_0$ leads to an optimal power split in the powertrain. The counterpart is that the state evolution is not controlled. Therefore several iterations are required to achieve a prescribed final state of charge, so the driving cycle needs to be a priori known (non causal approach).

A constant state-of-charge set point SOC_{sp} is considered. The main idea is to periodically modify the value of the Lagrange parameter $\widehat{\lambda_0}$ according to the state error and the power demand P_{DEM}. The principle is illustrated fig. 7.

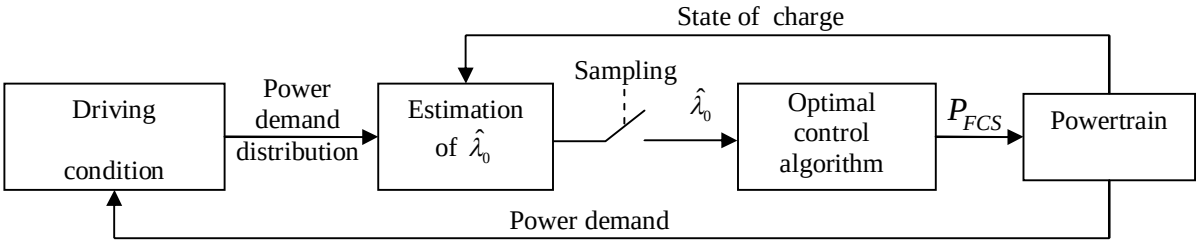

Fig. 7. Principle of the real time strategy.

Several strategies have been proposed to adapt the controller using past driving information. For example, /Jeon et al. 2002/ consider several driving patterns and an optimized controller for each pattern. During real time driving condition, the pattern that matches the actual driving is recognized using a neural network and the corresponding controller is used. As the database is finite, there is no possibility to ensure that it covers the actual driving condition.

Others strategies use an algorithm similar to the "*offline optimization*" *algorithm* with an adjustable Lagrange parameter $\widehat{\lambda_0}$. Considering non constant $\widehat{\lambda_0}$ leads obviously to a sub-optimal solution, but this approach allows controlling the state of charge. This kind of control strategy is often referred to as Equivalent Consumption Minimization Strategy /Sciaretta et al. 2004/. In particular, the Adaptive-ECMS /Musardo et al. 2005/ uses a time ordered prediction of the future power demand. This prediction is very hard /Bartholomaeus et al. 2008/ due to, for example, traffic disturbances or driver's behavior. In /Musardo et al. 2004/ authors noticed that it is difficult to work with a horizon prediction longer than 20 seconds.

The key point with the proposed control strategy is that the *time ordered* prediction of the future power demand is not necessary. According to equation (20) it is clear that only the prediction of their *distribution* is required. Therefore, it is not important to know *when* a specific power demand will be done (it would remain in a very tough prediction to realize for more than few seconds), only the future *global* condition of driving is mandatory.

According to the available information (GPS with digital map, etc), the prediction may be more or less complex. It is assumed that no other information than the past power demand is available, therefore the following simple prediction is proposed: the *distribution* of future power demand will be equal to the *distribution* of the past one over the last N_{adapt} samples.

Using the definition introduced in (20), defining $\hat{n}_i$, $i = 1..C$, the distribution of the future $P_{DEM}(k)$, $k \in \left[i+1, i+N_{adapt} \right]$ and n_i, $i = 1..C$, the distribution of the past power demand $P_{DEM}(k)$, $k \in \left[i-N_{adapt}, i \right]$, the proposed assumption is a zero-order estimation updated every N_{adapt} samples:

$$\hat{n}_i = n_i \tag{21}$$

Of course, more complex algorithms may be used for ~~the~~ prediction, but this simple and computational efficient prediction still provides quite interesting results in terms of fuel consumption.

At the sample i, for a given value of $\hat{\lambda}_0$, the state of charge estimation at the end of the prediction horizon is:

$$\widehat{SOC}\left(i+N_{adapt}\right) = SOC(i) + \hat{f}\left(\hat{\lambda}_0\right) \tag{22}$$

With $\hat{f}\left(\hat{\lambda}_0\right) = \frac{T_s}{X_{\max}} \cdot \sum_{i=1}^{C} n_i \cdot Q\left(P_{DEM}^i - \Pi\left(P_{DEM}^i, \hat{\lambda}_0\right)\right)$ and C the number of bins.

And finally, the value of $\hat{\lambda}_0$ that allows reaching the state of charge set point SOC_{sp} at the end of the prediction horizon is solution of:

$$\hat{f}\left(\hat{\lambda}_0\right) = SOC_{sp} - SOC(i) \tag{23}$$

Solution of (23) is found using a simple dichotic search. Therefore, the control strategy, called λ_{adapt}, is defined as:

Every N_{adapt} samples

  1 – Compute the power distribution n_i of the last N_{adapt} samples

  2 – Estimate $\hat{\lambda}_0$ such as $\hat{f}\left(\hat{\lambda}_0\right) = SOC_{sp} - SOC(k)$

  with k the current sample.

end

A set of simulation results is shown in fig. 8. It concerns *Vehicle1* simulated using the simulation model *Model1* on the R3 driving cycle. Two control strategies are compared: The real time λ_{adapt} strategy and the "*offline optimization*" algorithm. For the λ_{adapt} strategy, the following parameters were chosen: $SOC_{sp} = 60\%$, a time step of $T_s = 1s$, and the number of samples $N_{adapt} = 120 \left(\Leftrightarrow 2\min \right)$. These parameters have been tuned in simulation on different driving conditions (urban, outer urban, highway, etc.). They realize a good compromise between fuel consumption and battery state of charge regulation.

It can be observed that the adaptable value $\hat{\lambda}_0$ varies only slightly around the value provided by the "*offline optimization*" algorithm. For the same state of charge balance (+3.5%), the hydrogen consumption for λ_{adapt} is $1.53 kg_{H_2} / 100 km$ and $1.49 kg_{H_2} / 100 km$ for the "*offline optimization*" algorithm. The consumption achieved with the real time strategy is only 3.5 % higher.

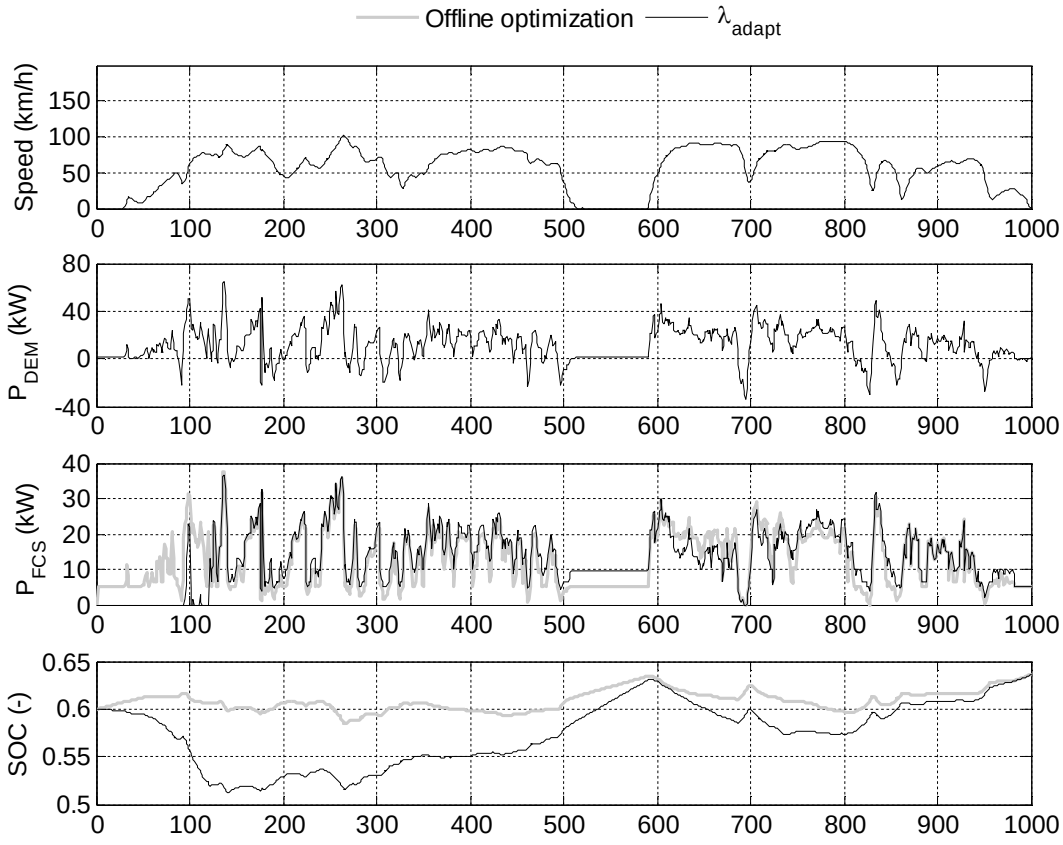

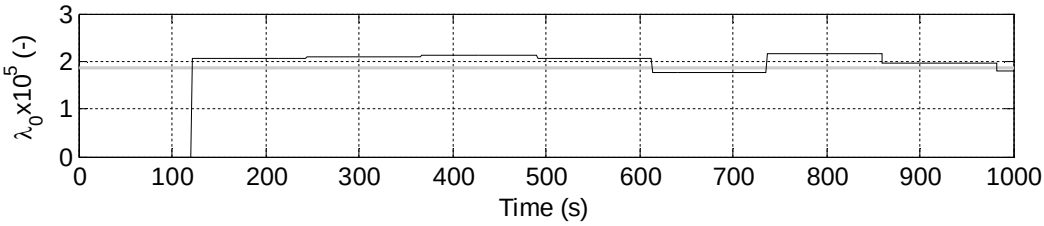

Fig. 8. Comparison between the λ_{adapt} strategy and the minimum principle results, R3 driving cycle, *Vehicle1*.

In order to emphasize the adaptation of the $\hat{\lambda}_0$ parameter, the λ_{adapt} control strategy is tested on a mixed driving cycle composed of urban-highway-urban driving conditions, fig. 9, keeping the same vehicle and control strategy tuning. The effect of the adaptation appears clearly: during the highway driving condition, the control strategy uses higher values of $\hat{\lambda}_0$. Using the λ_{adapt} control strategy, the state of charge remains close to its target $SOC_{sp} = 60\,\%$, the obtained overall state of charge variation is $SOC(N) - SOC(0) = 5.9\,\%$ and the corresponding hydrogen consumption is $1.69\ \mathrm{kg/100km}$.

Using the "*offline optimization*" algorithm based on the minimum principle and the a priori knowledge of the driving cycle, the solution leading to the same overall state of charge variation ($5.9\,\%$) has been also computed. It is obtained by choosing $\lambda_0 = 1.84 \cdot 10^{-5}$. The hydrogen consumption is $1.63\ \mathrm{kg/100km}$ and the state trajectory is also drawn fig. 9.

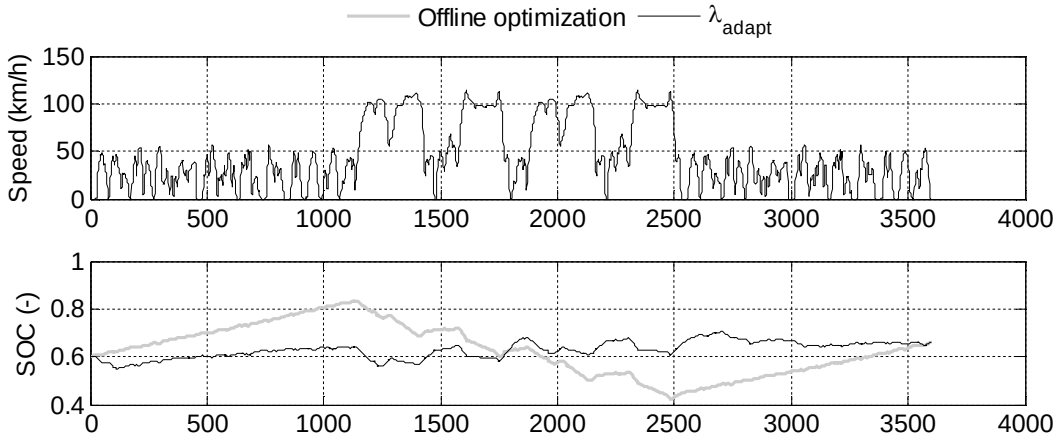

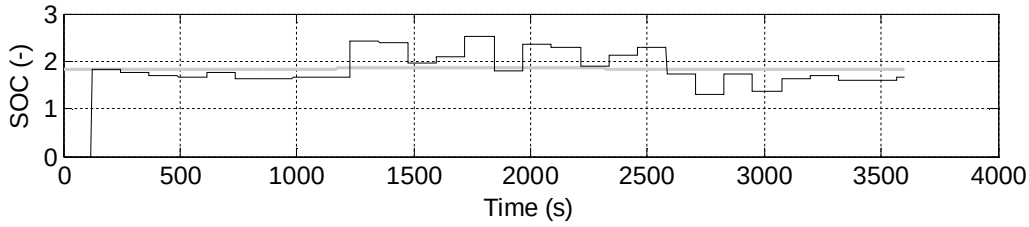

Fig. 9. Comparison between the λ_{adapt} and the optimal strategy, mixed driving cycle, *Vehicle1*.

The proposed real time on-line control strategy has also been experimentally tested. The experiments and results are described in the next section.

4. Experimental validation

To experimentally validate power management strategies of fuel cell hybrid vehicles, a low cost Hardware-in-the-Loop (HiL) test bench has been designed and realized. It emulates the power flows of a reduced scale powertrain of a hybrid fuel cell hybrid vehicle. This test bench is only used to compare the influence of the control algorithm on the energetic performances.

4.1. The test-bench

The HiL test bench, shown in Fig. 6, is split into two distinct sets:

1. **Emulation**: the vehicle is simulated in a computer and an electronic load reproduces the motor power demand.
2. **Hardware**: the core is a 600 W fuel cell system /Santis et al. 2004/; the energy buffer is either a battery or a super-capacitor. Simulation of “kinetic” energy recovery is also possible with the load (electronic load + power supply). A DC/DC converter controls the power delivered to the bus by the fuel cell system and the bus voltage is imposed by the energy buffer.

For the vehicle emulation, the power demand simulated on the computer is scaled according to the power capabilities of the hardware. The maximal power of the fuel cell system is limited to 600 W. For the 1500 kg light duty vehicle with a 40 kW fuel cell system used in simulation, this corresponds to a 66.6 scaling factor. A 12V/18Ah Lead Acid battery was employed as the energy buffer, corresponding with the scaling factor to a 14 kWh battery in the vehicle. In addition to the vehicle simulation, the computer is also used for system monitoring (fuel cell system temperature, stack pressure…), data acquisition and integrates high level controls such as the power management strategy.

In all experiments the temperature of the liquid coolant in the fuel cell stack was kept constant at 50 °C, i.e. no cold start or load dependent temperature changes were allowed. It should be noticed that thermal effects are important in fuel cells, temperature scales down not only with power but with size as well. So the obtained fuel consumption may not be exactly the same as those obtained with an actual fuel cell vehicle.

Therefore, the vehicle, namely *Vehicle2*, emulated with this test bench is similar to *Vehicle1* except for the battery technology and size (*Model2* : 14kWh lead acid battery vs *Model1*: 3.36 kWh Ni-Mh battery).

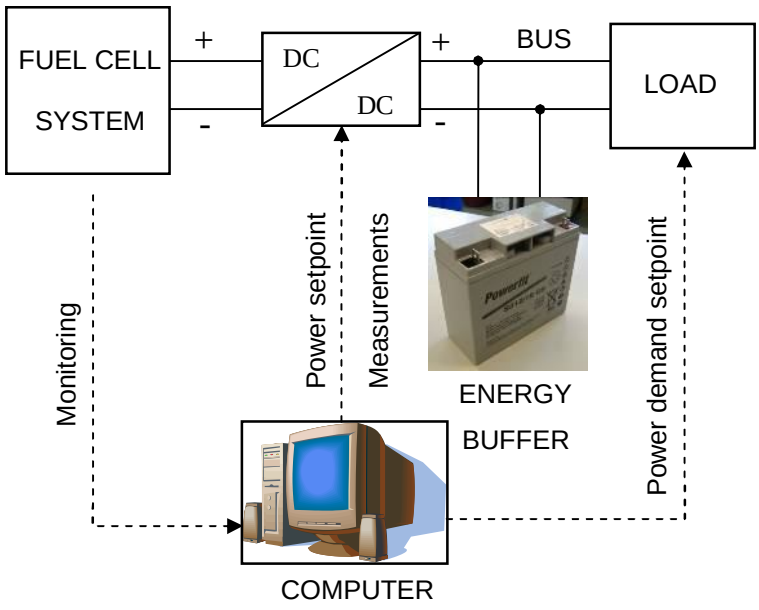

Fig. 10. Experimental setup of the hardware in the loop test bench emulating a hybrid electric vehicle. The load is bi-directional so also kinetic energy recovery can be simulated.

5. Results

As *Vehicle2* differs from *Vehicle1*, the parameters applied for the λ_{adapt} strategy are modified: $SOC_{sp} = 70\%$, $T_s = 1s$, and $N_{adapt} = 180 \left(\Leftrightarrow 3\min \right)$. These parameters were also tuned in simulation according to different driving cycles and they correspond to a good compromise between fuel consumption and SOC regulation. Fig. 11 shows the experimental results for the R3 driving cycle. The vehicle speed, the scaled power demand, the fuel cell system power, the state of charge of the battery and the evolution of $\hat{\lambda}_0$ are shown. The state of charge control is achieved by adapting the value of $\hat{\lambda}_0$, as shown in the plot at the bottom of fig. 11. The state of charge error remains acceptable (below 2 %).

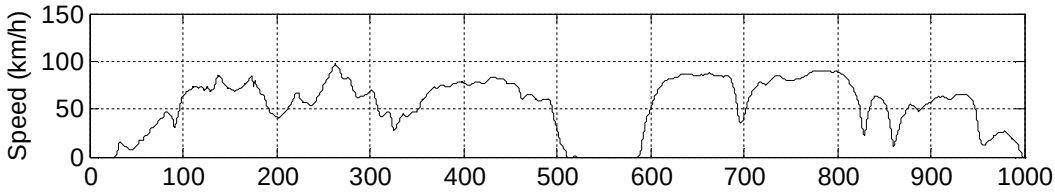

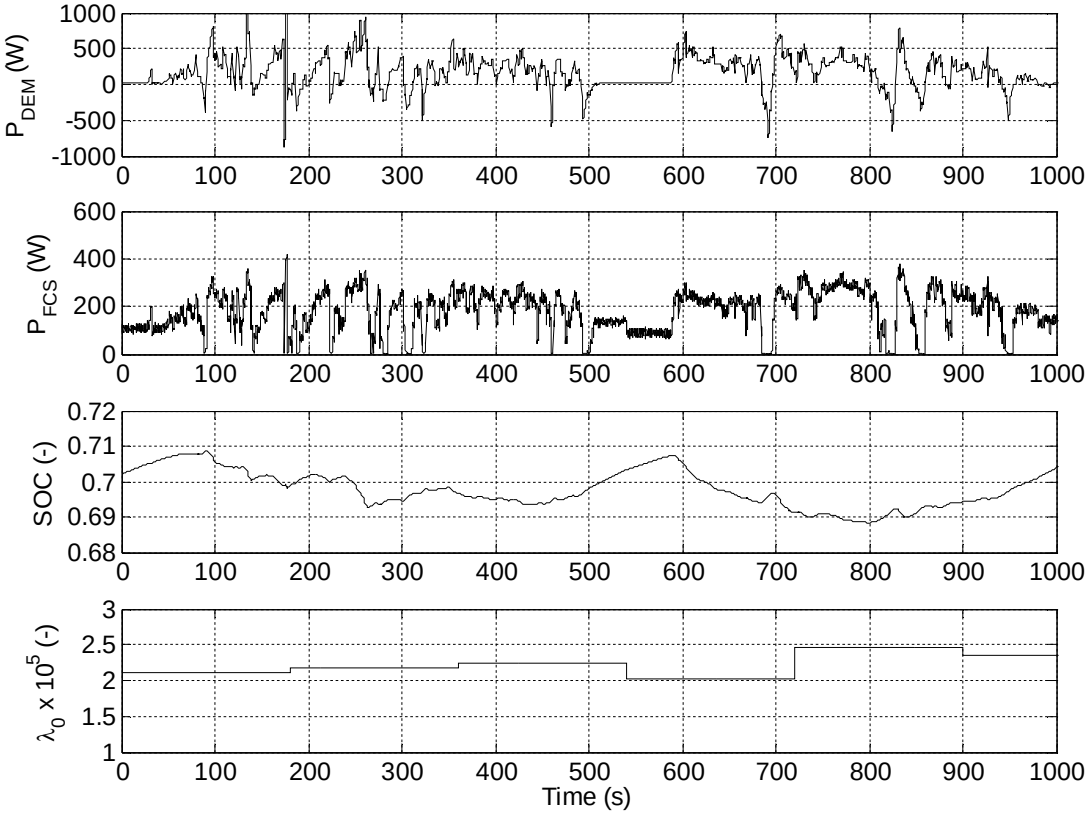

Fig. 11. Hardware in the loop (HiL) results for the λ_{adapt} strategy, outer-urban driving cycle, *Vehicle2*

In order to evaluate the quality of the λ_{adapt} strategy in term of hydrogen consumption, it has been compared to the Loss Minimization Strategy (LMS) /Seiler et Schröder 1998/. Amongst all the existing control algorithms, LMS is interesting since it considers an "unusual" criterion. At each sampling time the control value is chosen by minimizing the power losses in a hybrid powertrain. For LMS, the SOC regulation is done according to a sensitivity analysis. This strategy has been also intensively tuned on the simulation model of the test bench to make a comparison of the results as fair as possible, i.e. none of the strategies were advantaged during the experiments in term of consumption performances.

The hydrogen consumption of the λ_{adapt}, the LMS strategies and the "off line optimization" algorithm, were experimentally measured for the outer urban cycle R3. In fig. 12, the results are plotted as function of the state of charge balance. For negative SOC balances, the difference between the strategies is smaller because the energy mainly originates from the

battery and the influence of the strategy is reduced. At zero state of charge balance, the λ_{adapt} strategy provides 6 % better hydrogen consumption. At a positive SOC balance of 10%, the λ_{adapt} strategy provides 5.7 % better hydrogen consumption. For both driving cycle, the obtained results remain close to those obtained using the *"offline optimization"* algorithm.

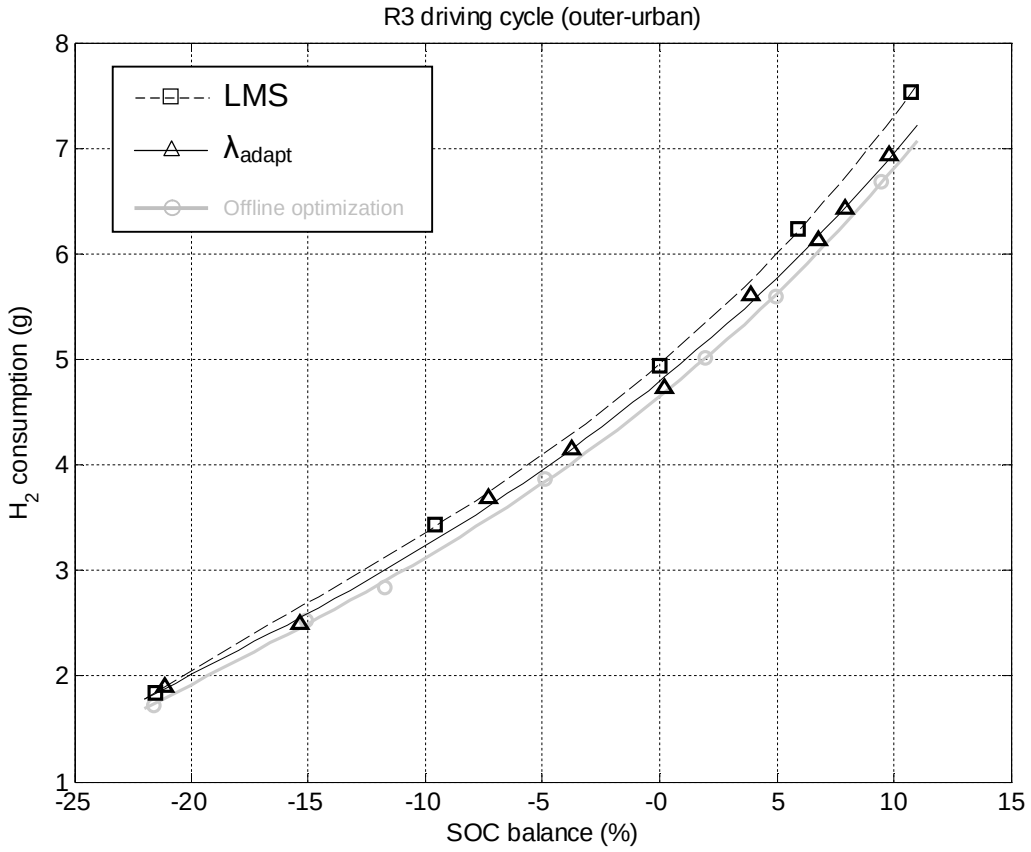

Fig. 12. Experimental results for outer-urban driving cycle (15.7 km, top) , *Vehicle2.*

6. Conclusion

The power management strategy of fuel cell hybrid vehicles has been investigated. An efficient real time control strategy has been derived from an optimal control algorithm. The optimization efforts rely on a simple but computationally exploitable powertrain model and the minimum principle.

To validate the proposed λ_{adapt} strategy, Hardware-in-the-Loop (HiL) experiments have been conducted. The HiL experiments were based on a 600W fuel cell system hybridized with a

lead acid battery. The λ_{adapt} strategy achieves a good fuel consumption economy both for simulations and experiments. In comparison with the LMS strategy (based on the instantaneous minimization of the power losses), the fuel consumption of λ_{adapt} is reduced at least by 4 %.

Further improvements of the λ_{adapt} strategy could be achieved by considering further parameters influencing the hydrogen consumption such as the evolution of the FCS temperature. Indeed, the FCS performances strongly depend on its temperature /Markel et al. 2003/ /Boettner et al. 2002/. To limit this influence, the HiL experiments were performed at a controlled and almost constant temperature of the stack, which actually does not represent real operating conditions in an automotive environment (cold start, stack temperature variation according to FCS load…). Further improvements of the proposed strategy are therefore possible.

7. Acknowledgment

The present research work has been supported by International Campus on Safety and Intermodality in Transportation, the Nord-Pas-de-Calais Region, the European Community, the Regional Delegation for Research and Technology, the Ministry of Higher Education and Research, and the National Center for Scientific Research. The authors gratefully acknowledge the support of these institutions and also the PSI (Paul Scherrer Institut).

References

André M., Joumard R., Vidona R., Tassela P., Perret P., *Real-world European driving cycles, for measuring pollutant emissions from high- and low-powered cars,* Atmospheric Environment , Vol. 40 (31), pp. 5944-5953, 2006.

Barrade P., **Rufer** A., *The use of supercapacitors for energy storage in traction systems,* IEEE Vehicle Power and Propulsion Conference, Paris, Octobre 2004.

Bartholomaeus R., Klingner M., Lehnert M., *Prediction of power demand for hybrid vehicles operating in fixed-route service*, Proceedings of the 17th World Congress The International Federation of Automatic Control Seoul, Korea, July 6-11, 2008.

Bauman J., **Mehrdad** M., *A Comparative Study of Fuel-Cell–Battery, Fuel-Cell–Ultracapacitor, and Fuel-Cell–Battery–Ultracapacitor Vehicles*, IEEE Transaction on Vehicular Technology, Vol. 57, No. 2, March 2008.

Bernard J., Delprat S., Büchi F.N., Guerra T.M., *Fuel Cell Hybrid Vehicles: Global optimization based on optimal control theory*, International Review of Electrical Engineering (I.R.E.E.), Vol. 1, n. 3. July-August 2006.

Bernard J., *Fuel Cell Hybrid Vehicles : powertrain sizing and power management strategies*, PhD Thesis, LAMIH UMR CNRS 8530, University of Valenciennes Et Du Hainaut-Cambrésis, December 2007.

Boettner D.D., Paganelli G., Guezennec Y.G., Rizzoni G., Moran M.J., *Proton Exchange Membrane (PEM) fuel cell system for automotive vehicle simulation and control*, Journal of Energy Resources Technology (Transactions of the ASME), Vol. 124 (1), pp. 20-27, Mars 2002.

Dalvi a., Guay M, *Control and real-time optimization of an automotive hybrid fuel cell power system*, Control Engineering Practice, Volume 17, Issue 8, August 2009, Pages 924-938.

Delprat S., Lauber J., Guerra T.M., Rimaux J., *Control of a parallel hybrid powertrain : Optimal Control*, IEEE Transactions on Vehicular Technology, Vol. 53 (3), pp. 872-881, 2004.

Dietrich P., Büchi F., Tsukada A., Bärtschi M., Kötz R., Scherer G.G., Rodatz P., Garcia O., Ruge M., Wollenberg M., Lück P., Wiartalla A., Schönfelder C., Schneuwly A., Barrade P., *Hy.Power-A technology*

platform combining a fuel cell system and a supercapacitor, Handbook of Fuel Cells – Fundamentals, technology and Applications, Volume 4, Part 11, pp. 1184-1198, 2003.

Gruber J.K., Doll M., Bordons C., *Design and experimental validation of a constrained MPC for the air feed of a fuel cell*, Control Engineering Practice, Volume 17, Issue 8, August 2009, Pages 874-885.

Guezennec Y., Ta-Young Choi, Paganelli G., Rizzoni G., *Supervisory control of fuel cell vehicles and its link to overall system efficiency and low-level control requirements,* Proceedings of the American Control Conference 2003, June 2003, Volume: 3, pp 2055- 206,1 vol.3.

Haraldsson K., **Wipke** K., *Evaluating PEM fuel cell system models,* Journal of Power Sources , n°126 (2004) pp 88–97.

Jeon S., Jo T., Park Y., Lee J., *Multi-Mode Driving Control of a Parallel Hybrid Electric Vehicle Using Driving Pattern Recognition*, Journal of Dynamic Systems, Measurement, and Control, March 2002, Vol. 124, pp.141-149.

Jeong K.S., **Oh** B.S., *Fuel economy and life-cost analysis of a fuel cell hybrid vehicle*, Journal of Power Source, Vol. 105, pp. 58-65, 2002.

Markel T., Zolot M., Wipke K.B., Pesaram A.A., *Energy storage requirements for hybrid fuel cell vehicles*, Advanced Automotive Battery Conference, Nice, France, Juin 2003.

Musardo C., Rizzoni G., Staccia B., *A-ECMS: An Adaptive Algorithm for Hybrid Electric Vehicle Energy Management*, Proceedings of the 44th IEEE Conference on Decision and Control, and the European Control Conference 2005, Seville, Spain, December 12-15, 2005.

Musardo C., Staccia B., Bittanti S., Guezennec Y., Guzzela L., Rizzoni G., *An adaptive algorithm for hybrid electric vehicles energy management*, FISITA World Automotive Congress, Barcelona (Spain), 2004 (available online http://www.fisita.com/education/congress/SCpapers/sc34.pdf).

Pontryagin L.S., Boltyanski V.G., Gamkrelidze R.V., Mischenko E.F., *The mathematical theory of optimal processes*, Interscience, 1962.

Rodatz P., Paganelli G., Sciarretta A., Guzzella L., *Optimal power management of an experimental fuel cell/supercapacitor-powered hybrid vehicle*, Control Engineering Practice, vol. 13, pp. 41-53, 2005.

Santis M., Schmid D., Ruge M., Freunberger S., Büchi F.N., *Modular Stack-Internal Air Humidification Concept-Verification in a 1 kW Stack Fuel Cells*, Volume 4, Issue 3, pp. 214-218, August 2004,

Sciarretta A., **Guzzella** L., *Control of Hybrid Electric Vehicles - A Survey of Optimal Energy-Management Strategies*, IEEE Control Systems Magazine, Vol. 27 (2), pp. 60-70, 2007.

Sciarretta A., Back M., Guzzella L., *Optimal Control of Parallel Hybrid Electric Vehicles*, IEEE Transactions on Control Systems Technology, VOL. 12, NO. 3, MAY 2004.

Scordia J., *Systematic approach of the sizing optimization and the elaboration of energy management laws for an hybrid vehicle*, PhD thesis, Université Henri Poincaré, Nancy, France, 2004.

Serrao L., Onori S., Rizzoni G., *ECMS As a Realization of Pontryagin's Minimum Principle for HEV Control*, 2009 American Control Conference, June 10-12, 2009, St. Louis, Missouri, USA.

Seiler J., Schröder D., *Hybrid vehicle operating strategies*, Electric Vehicle Symposium EVS15, Bruxelles, 1998.

Spotnitz R., *Advanced EV and HEV Batteries*, IEEE Vehicle and Power Propulsion Conference, Chicago, September 2005.

Wee J.H., *Applications of proton exchange membrane fuel cell systems*, Renewable and Sustainable Energy Reviews, Vol. 11, pp. 1720-1738, 2007.

Yamaguchi J., *Preparing for the hydrogen age, Automotive Engineering International*, Vol. 111, n° 10, pp. 8-10, October 2003.